FE-3800-10
Dist. Category UC-90C

MATERIALS RESEARCH FOR CLEAN UTILIZATION OF COAL

QUARTERLY PROGRESS REPORT
October 1 - December 31, 1976
(JANUARY)
77

Samuel J. Schneider
Project Manager

Institute for Materials Research
National Bureau of Standards
Washington, D. C.   20234

PREPARED FOR THE UNITED STATES
ENERGY RESEARCH AND DEVELOPMENT ADMINISTRATION

Under Contract No. E(49-1)-3800

TABLE OF CONTENTS

I. OBJECTIVE AND SCOPE OF WORK

Coal Gasification processes require the handling and containment of corrosive gases and liquids at high temperature and pressures, and also the handling of flowing coal particles in this environment. These severe environments cause materials failures which inhibit successful and long-time operation of the gasification systems. The project entails investigations on the wear, corrosion, chemical degradation, fracture, and deformation processes which lead to the breakdown of metals and ceramics currently being utilized in pilot plants. Studies will also be carried out on new candidate materials considered for improved performance. Special emphasis will be devoted to the development of test methods, especially short-time procedures, to evaluate the durability of materials in the gasification environments. These methods will focus on wear, impact erosion, stress corrosion, strength, deformation, slow crack growth and chemical degradation of refractories. A system has been initiated to abstract and compile all significant operating incidents from coal conversion plants. This program will provide a central information center where problems of common interest can be identified and analyzed to avoid unnecessary failures and lead to the selection of improved materials for coal conversion and utilization. Active consultation to ERDA and associated contractors will be provided as reqested.

II. SUMMARY OF PROGRESS TO DATE

The summary of progress is contained in the individual task progress and plans - Section III.

III. DETAILED DESCRIPTION OF TECHNICAL PROGRESS

1. Metal Corrosion

a. Constant Strain-Rate Test (G. M. Ugiansky and C. E. Johnson, 312.04)

Progress: The investigation of the cause of embrittlement of type 310 stainless steel at elevated temperatures and at slow strain rates has continued. Comparisons were made between embrittled specimens and non-embrittled specimens of 310 SS and other alloys. Microscopic examination of the cross-sections of 310, 310 S, 347 SS, and Incoloy 800 tested at 540°C (1000°F) in H_2S plus steam or H_2S saturated with water vapor at room temperature revealed internal intergranular cracking in 310 SS that was tested at a strain rate of 3.6×10^{-6} s^{-1} as well as surface cracks progressing into the bulk of the specimen (Fig. 1); whereas, a 310 SS specimen tested at the faster strain rate of 1.3×10^{-4} s^{-1} (in the same environment and at the same temperature) shows a ductile type fracture with no internal or surface cracks (Fig. 2). Surface cracking of 310 SS was detected in specimens up to a maximum strain rate of 7.2×10^{-6} s^{-1} when tested at 540°C (1000°F) (Fig. 3). The necking which can be seen when Fig. 1 and Fig. 3 are compared shows that the specimen in Fig. 3 is still somewhat ductile inspite of the surface cracking. At a slower strain rate of 8.4×10^{-7} s^{-1}, the 310 SS (Fig. 4) does not exhibit as much internal intergranular cracking but does reveal larger surface cracks progressing farther into the bulk of the specimen than in the 310 SS specimen tested at the higher strain rate of 3.6×10^{-6} s^{-1} (Fig. 1). Precipitates were seen in the grain boundaries of all the 310 SS specimens regardless of the strain rate at which it was tested. Fig. 5 shows a representative area of grains with grain boundary precipitates in the 310 SS specimens.

Internal intergranular cracking was observed in 310 S stainless steel but only when tested at the slow strain rate of 8.4×10^{-7} s^{-1} (Fig. 6). Precipitates were also present in the grain boundaries in all of the 310 S specimens regardless of the strain rate at which they were tested, but the precipitates seemed to be more pronounced in the specimen tested at the slow strain rate of 8.4×10^{-7} s^{-1} (Fig. 7). In the 310 S, with a lower carbon content than 310, there is less carbon present to diffuse to the grain boundaries to form the precipitates; and, therefore, the formation of the precipitates requires longer times. No internal cracking was revealed for any of the 347 SS specimens over the range of strain rates tested. No surface cracking was apparent even though several of the specimens showed tool marks on the surface. On the 347 SS specimen (Fig. 8) run at the slow strain rate of 8.4×10^{-7} s^{-1}, some of the tool marks opened up in the necked-down area but were shallow and blunt. However, all subsequent specimens tested had tool marks removed by polishing the surface of the reduced area.

No surface cracking and little, if any, internal intergranular cracking could be detected in the Incoloy 800 over the range of strain rates tested. Only the Incoloy 800 specimen tested at 8.4×10^{-7} s^{-1} (Fig. 9) showed a slight indication of internal cracking. There did appear to be some formation of precipitates in the grain boundaries of Incoloy 800 run at strain rates of 7.3×10^{-6} s^{-1} and at 8.4×10^{-7} s^{-1} (Fig. 10).

A determination of the origin of the crack process would help identify the mechanism of cracking, especially with respect to the influence or lack of same of the environment on cracking. However, a thick corrosion product layer on the fracture surface of the 310 stainless steel specimens tested at 540°C (1000°F) in H_2S plus steam or H_2S saturated with water vapor at room temperature prevented a detailed fractographic study of those specimens. However, microscopic examination of the fracture surface of type 310 SS tested in dry helium, argon, and vacuum (house vacuum line, 34 Torr, 4500 Pa) at 540°C (1000°F) and at strain rates $\simeq 1 \times 10^{-6}$ s^{-1} have revealed evidence of brittle fracture (intergranular cracks and faceted structure) near the original surface of the specimen with ductile fracture (dimples) at the center of the fracture surface and on the shear lip. This indicates that the origin of the crack is at the metal/environment interface and not at the center of the specimen — further evidence that the cracking is by an environmental mechanism. Fig. 11 shows a representative fracture surface of a 310 SS specimen tested at 540°C (1000°F) and $\simeq 1 \times 10^{-6}$ s^{-1}. Fig. 12 is a photomicrograph of the flat area near edge of fracture surface of Fig. 11. Note the intergranular cracks and faceted structure. Fig. 13 is a photomicrograph of an area near the center of the fracture surface of Fig. 11. Note the dimpled structure indicative of ductile fracture.

To clarify the mechanism of failure, further methods of eliminating the oxygen and water vapor from the test environment are being applied. New flanges were made for the test chamber to facilitate the test of 310 SS in a somewhat better vacuum (2×10^{-2} Torr, 2.66 Pa) than that in which the previously tested specimens were tested (house vacuum). Upon completion of the test at $\simeq 1 \times 10^{-5}$ s^{-1}, the surface of the specimen was oxidized, and the same brittle type fracture occurred with secondary surface cracks. There was apparently enough oxygen and/or water vapor present to cause cracking.

Another test was run on 310 SS. This time a reducing environment (H_2) was used. It was thought that the reducing atmosphere of H_2 would prevent or limit the effect of oxygen. The H_2 was handled in the following manner: the H_2 gas was passed through a liquid N_2 trap, through copper turnings at 565°C (1050°F), through another liquid N_2 trap, through the test chamber at a low positive pressure, through another liquid N_2 trap, and through a H_2O bubbler that was vented directed to the exhaust system. This test run was made at 540°C

3

(1000°F) at a strain rate of 8.4 X 10^{-7} s^{-1}. Some blue oxide was still present on the specimen after the test, but the amount of oxide was the least that has been seen for any tests in any environment. The fracture was still of the brittle type with some secondary cracking. The reduction in area (23.3%) was higher for this specimen, tested in H_2, than for other 310 SS specimens tested in other environments (17-19%) with the exception of one 310 SS specimen tested at 540°C (1000°F) at a strain rate of 8.4 X 10^{-7} s^{-1} in ultra pure He (25%).

Testing of the alloys has been started at a strain rate of 1 X 10^{-7} s^{-1} in H_2S saturated with water vapor at room temperature at 540°C (1000°F).

Gas mixtures of CO, CO_2, H_2, and CH_4 have been prepared and analyzed but have not been shipped since they will be used to calibrate flow-meters that have been ordered. The gases and flow meters are scheduled to be delivered in two weeks.

Plans: Complete tests of types 310, 310 S, 347 stainless steel and Incoloy 800 at the very low strain rate of 1 X 10^{-7} s^{-1} in H_2S saturated with water vapor at room temperature at 540°C (1000°F), while continuing the search for the cause of failure in the 310 SS.

growth rate as a function of K_I or the stress-intensity threshold level below which crack growth rate does not occur can be readily determined. For this configuration of specimen, the stress intensity (K_I) is then given in terms of the crack length (a), the specimen height (H), the specimen arm displacement due to the wedge (V) and the modulus of the specimen (E) as follows: (ref. 1)

$$K_I = \frac{EV}{\sqrt{H}} \left[\frac{3.46 + 2.38\,(H/a)}{7.97\,\left(\frac{a}{H}\right)^2 + 16.48\,\left(\frac{a}{H}\right) + 11.32} \right]$$

This equation shows that the stress-intensity (K_I), is relatively insensitive to crack length (a) for a/H values greater than about 3, so that accurate values of K_I are determined without requiring extremely accurate crack length (a), measurements.

For use at elevated temperature, the above equation for stress-intensity, K_I, must take into account the following effects:

1) Decrease in elastic modulus, E, with increase in temperature.

2) Increase in arm displacement, V, due to thermal expansion.

3) Increase in effective crack length, a_{eH}, due to increase in plastic zone size caused by the decrease in the yield strength of the specimen with increase in temperature.

4) Decrease in the measurement capacity (maximum stress-intensity that can be measured) for a given size specimen due to decrease in the yield strength of the specimen material.

The equation for stress-intensity given above was modified to take into account these effects. For a wedge-loaded, double cantilever beam specimen loaded at room temperature to a stress-intensity level designated $(K_I)_o$, the change in stress-intensity when the temperature is increased to some value T is $(K_I)_T$, where the ratio $(K_I)_T/(K_I)_o$ is:

$$\frac{(K_I)_T}{(K_I)_o} = \frac{E_T}{E_o}\,\frac{V_T}{V_o}\left(\frac{f\left(\frac{a_T}{H_T}\right)}{f\left(\frac{a_o}{H_o}\right)}\right)$$

where:

    E_T - modulus of elasticity of specimen at temperature T.

    E_o - modulus of elasticity of specimen at room temperature.

V_T - arm displacement at temperature T.

V_o - arm displacement at room temperature.

$$f\left(\frac{a_T}{H_T}\right) = \left[\frac{3.46 + 2.38\left(\frac{H_T}{a_T}\right)}{7.97\left(\frac{a_T}{H_T}\right)^2 + 16.48\left(\frac{a_T}{H_T}\right) + 11.32}\right]$$

where a_T and H_T are the crack length and specimen height at temperature T
$f\left(\frac{a_o}{H_o}\right)$ is the same function for crack length, a_o, and specimen height, H_o
at room temperature.

It is desirable for temperature to have as small an effect as possible on the stress-intensity. That is, for the ratio $\frac{K_I}{K_o}$ to be approximately 1 over a wide range of temperature. To achieve this, the effect of temperature on each of the terms in the above equation was investigated to select values than minimize the effect of temperature on the ratio $\frac{K_T}{K_o}$. The effect of temperature on crack length, a, and specimen height, H, is relatively small and since for a/H ratios greater than about 3, the stress intensity K is relatively unsensitive to a/H, the ratio
$f\left(\frac{a_T}{H_T}\right)/f\left(\frac{a_o}{H_o}\right)$ is approximately 1.0. Therefore the above equation is reduced to:

$$\frac{K_T}{K_o} \cong \frac{E_T}{E_o}\frac{V_T}{V_o}$$

where:

$$V_o = h_w - h_s$$

$$V_T = [h_w(1 + \alpha_w)(T - T_o)] - [h_s(1 + \alpha_s)(T - T_o)]$$

h_w - height of wedge at loading point

h_s - height of slot in specimen

α_w - coefficient of thermal expansion of wedge

α_s - coefficient of thermal expansion of specimen

20

T_o - reference temperature (taken as room temperature)

T - test temperature.

Therefore:

$$\frac{K_T}{K_o} \approx \frac{E_T}{E_o} \; [1 + (\frac{h_w \alpha_w - h_o \alpha_s}{h_w - h_o}) \; (T - T_o)]$$

For a given test material the choice of wedge size and material is chosen so that as nearly as possible the thermal expansion of the wedge compensates for the decrease in modulus of elasticity of the test specimen with temperature.

Plans: The analysis of the effect of thermal expansion, change in modulus of elasticity with temperature and change in plastic zone size with temperature will be completed. For each of the specific materials of interest for use at high temperature, the elastic stress-intensity factor will be calculated for temperatures up to 2000°F and the maximum stress-intensity for use of linear elastic fracture mechanics will be established.

Reference:

1. B. F. Brown, Stress-Corrosion Cracking in High Strength Steels and in Titanium and Aluminum Alloys, Naval Research Laboratory, 1972 Chap. 2.

2. Ceramic Deformation, Fracture and Erosion (E. R. Fuller, S. M. Wiederhorn, C. R. Robbins and D. E. Roberts, 313.05)

Progress: The main effort of the past quarter has been the design and construction of new test equipment. In addition, the mechanical properties and mineral composition of two laboratory mixtures of castable refractories (high and low alumina calcium-aluminate castables) have been studied after elevated temperature-pressure exposure, and the erosive behavior of a phosphate-bonded refractory has been examined.

A great deal of progress has been made on the construction of the apparatus for mechanical properties testing in simulated coal gasification environ-- ments. The outer pressure shell for this apparatus has been constructed. A Radiographic inspection of the original garth welds revealed two flaws which have been repaired. The design of the interior of the apparatus has been completed, detailed mechanical drawings have been prepared, and the components are presently being constructed in the NBS Machine Shop. A base, which will support the pressure vessel, has been designed and is also being constructed. The base will provide explosion protection, and ventilation for the pressure vessel. Other systems and components (such as: temperature controllers, refractory insulation, a pressure-balance controller, and a chain hoist) have been ordered and most have arrived.

The equipment for particle erosion has been enclosed and connected to an exhaust system. The enclosure will satisfy the NBS Safety Office rules on dust/particle hazards and will permit injection of additional gaseous components into the stream of eroding particles. In addition, a ventila- tion system for exhausting explosive and/or noxious gases from the three pressure vessel systems and the gas tank storage rack has been designed. A spark-proof and corrosion resistant exhaust fan for this system has been ordered, and received, and will be installed shortly.

High-temperature exposure experiments were initiated in a pressure vessel recently purchased by NBS. The unit, has been plagued with a number of minor problems (pressure leaks, a faulty temperature controller, a faulty water pump, and a defective pressure gauge isolation system) which have slowed the collection of data. Most of these problems have now been overcome and specimens of both a high alumina (∼95%) and a low alumina (∼56%), calcium-aluminate refractory castable have been exposed to steam at 1000 psig (7.0 MPa) at temperatures running from 310°C (590°F) to 910°C (1670°F). After exposure the following properties have been examined: flexural and compressive strengths at two rates of loading; erosive wear by particle impingement; porosity; mineral phases; and microstructural morphology. Results are still preliminary at this time.

22

Plans: Construction will continue on the apparatus for mechanical properties testing in simulated coal gasification environments. Completion of the main portions of this apparatus and "check-out" of the heat zone is anticipated in the next quarter. Construction of the ventilation system should begin and be substantially completed in the next quarter. Exposure studies will continue with gaseous compositions (molar percent) of 70% water and 30% carbon dioxide and of 30% water and 70% carbon dioxide at 1000 psig total pressure. Upon completion of the ventilation system, mixtures with carbon monoxide will be considered. Work to characterize the erosion behavior of three basic castable compositions (a 95% alumina, a 56% alumina and a phosphate bonded refractory) as a function of temperature, particle velocity and impingement angle will be completed, and studies on the effect of particle size on erosion rate will be started.

3. Chemical Degradation

a. Reactions and Transformations (F. Mauer and C. R. Robbins, 313.06)

Progress: During this quarter work on the design and construction of apparatus for x-ray examination of refractory castables under simulated gasification conditions was continued. While the pressure vessel was under construction in the NBS Instrument Shops, design of the x-ray goniometer (for mounting and aligning the pressure vessel on the x-ray apparatus) was completed and construction was begun. The pressure vessel and goniometer are expected to be completed by about January 15, 1977.

All of the components for the gas manifold have been purchased. Gases will be introduced through a gauge block that includes a needle valve, pressure gauge and rupture disc. Water will be introduced separately from a 40 ml cylinder pressurized with N_2 gas. A second 40 ml cylinder has been included in the system so that a sample of the atmosphere can be withdrawn for analysis.

Additional samples have been obtained for use in preparing standard x-ray patterns by the energy dispersive diffraction method. A calculator program has been written which can be used to convert d-spacings and intensities from a conventional powder diffraction pattern to channel number and counts (peak and background) for the energy dispersive diffraction pattern. This program is being used in the interpretation of the patterns being prepared for use as working standards.

Plans: Construction of major components is expected to be completed during January so that the system can be assembled during February and used for calibration runs. In situ x-ray diffraction measurements (subtask 3a-3) are expected to begin by April 1, 1977, as proposed in our original work statement.

b. Slag Characterization   (W.S. Brower, J.L. Waring, 313.03 and
                             D.H. Blackburn, 313.02)

Progress: The viscosities of synthetic slags (one modeled after Montana
Rosebud Coal Ash analyses and the other modeled after Pittsburgh Seam
Coal Ash) have been measured at ambient pressure over the temperature
range of 1300°C to 1600°C (Figure 1a and 1b). The compositions are given
in Table 1.

Table 1. Slag Compositions

Rosebud		Pittsburgh Seam	
SiO_2	42.10 wt%	SiO_2	49.0 wt%
Al_2O_3	19.50	Al_2O_3	26.0
Fe_2O_3	7.11	Fe_2O_3	19.0
CaO	24.48	CaO	3.5
Na_2O	0.21	Na_2O	0.6
K_2O	0.10	K_2O	1.2
MgO	5.50	MgO	0.7
TiO_2	0.90		

The gear motor for crucible rotation has been received and the torsion
wire suspensions have been calibrated with two fluids of known viscosity
using two different "drag cup geometries" (Figure 2).

Preliminary tests have been run in an autoclave operating at 30 psig
steam pressure using a platinum strip heater with a radiating area
of 15 square inches to evaluate the effect of steam pressure on the
heater temperature at a constant power level. A 20% reduction in
temperature was observed from ambient pressure to 30 psig (Figure 3)
at 800°C.

Plans: While the pressure vessel construction is being completed a
series of synthetic slags with systematically varying composition will
be formulated and the viscosities measured is a function of temperature
and compared to viscosity data obtained from predictive equations. In
the next quarter the vessel construction should be complete.

Figure 1a. Viscosity of synthetic slag vs temperature.

Rosebud Type Coal Ash

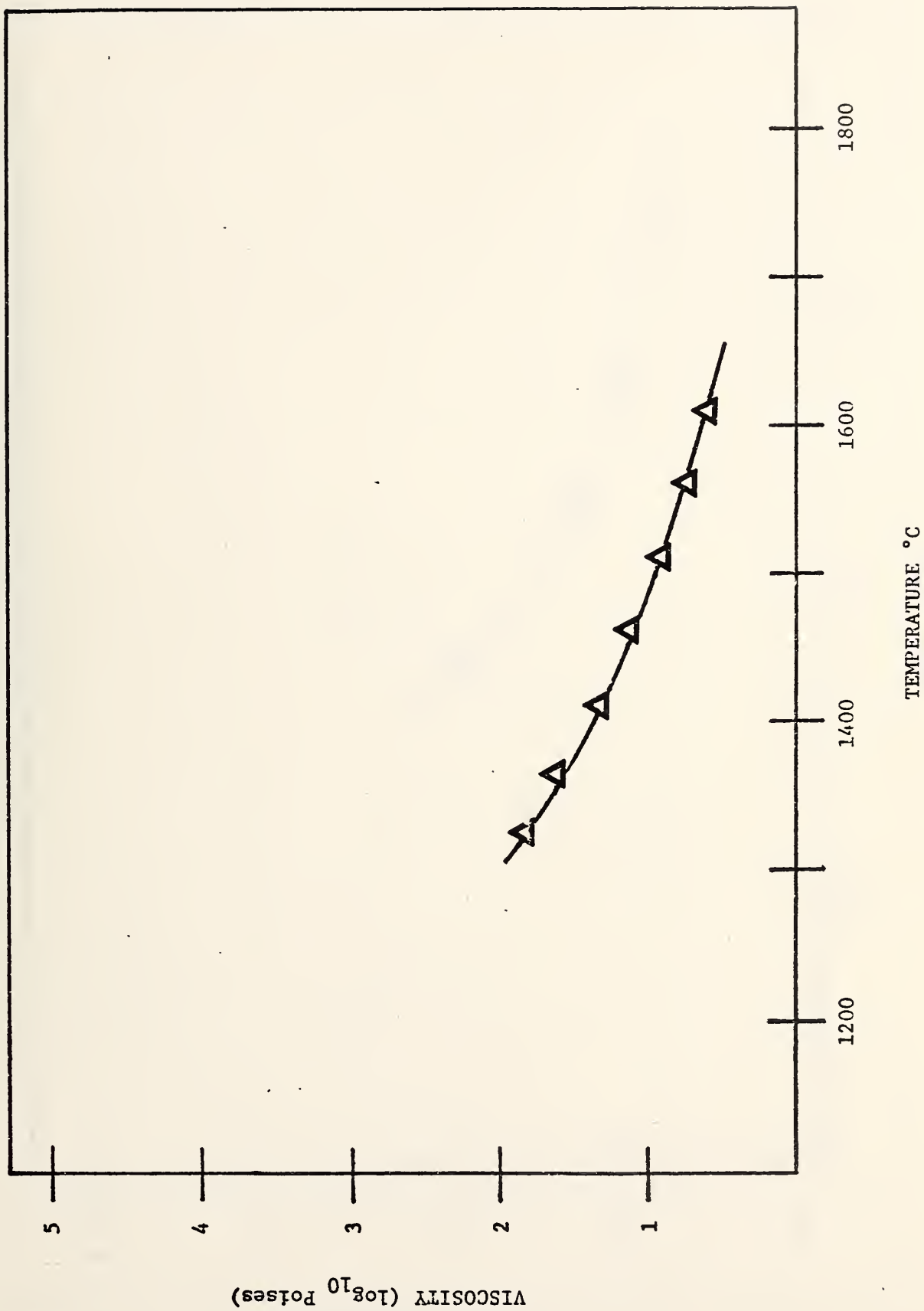VISCOSITY ($\log_{10}$ Poises)

TEMPERATURE °C

25

Figure 1b. Viscosity of synthetic slag vs temperature.
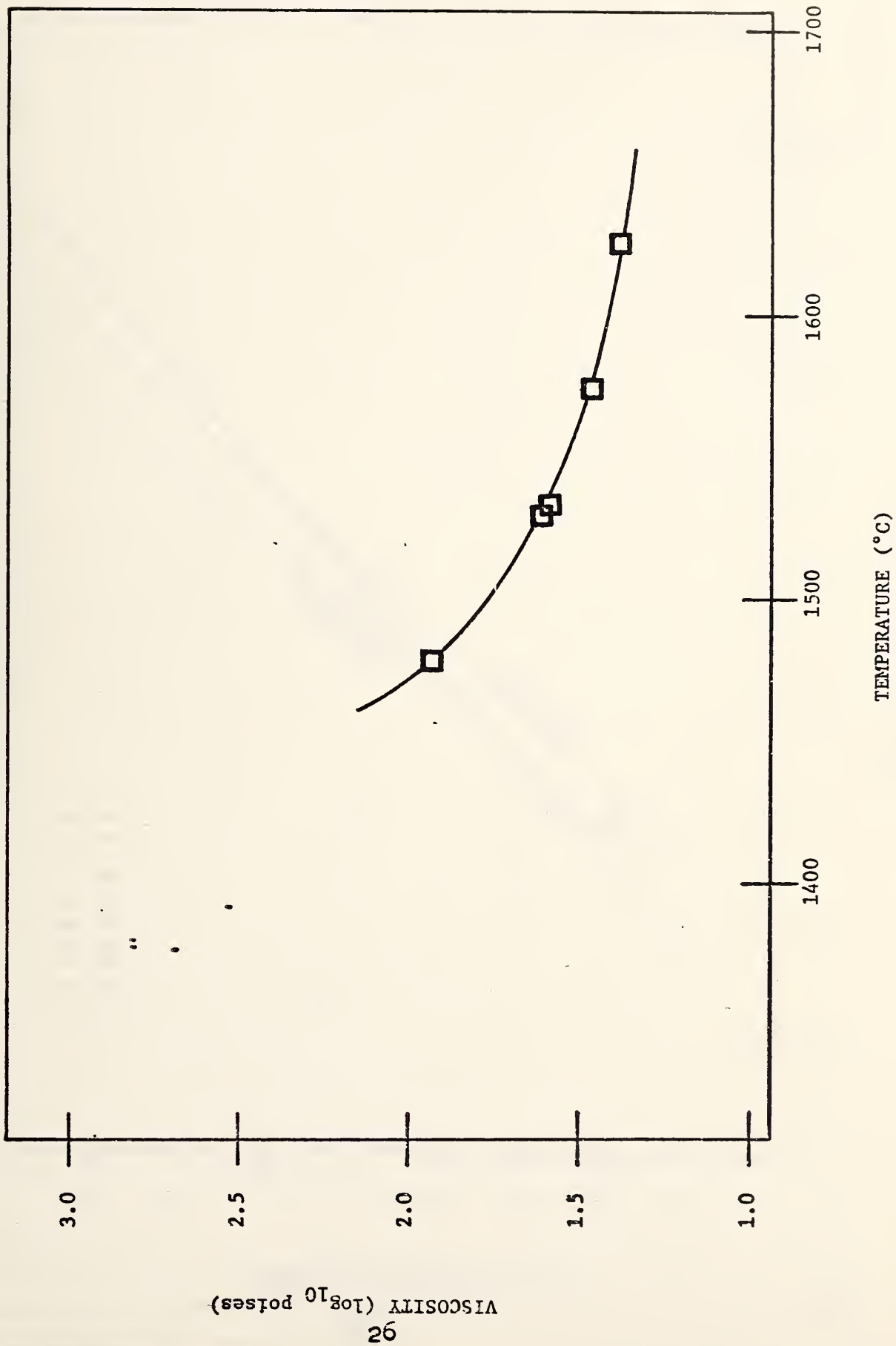Pittsburgh Seam Type Coal Ash
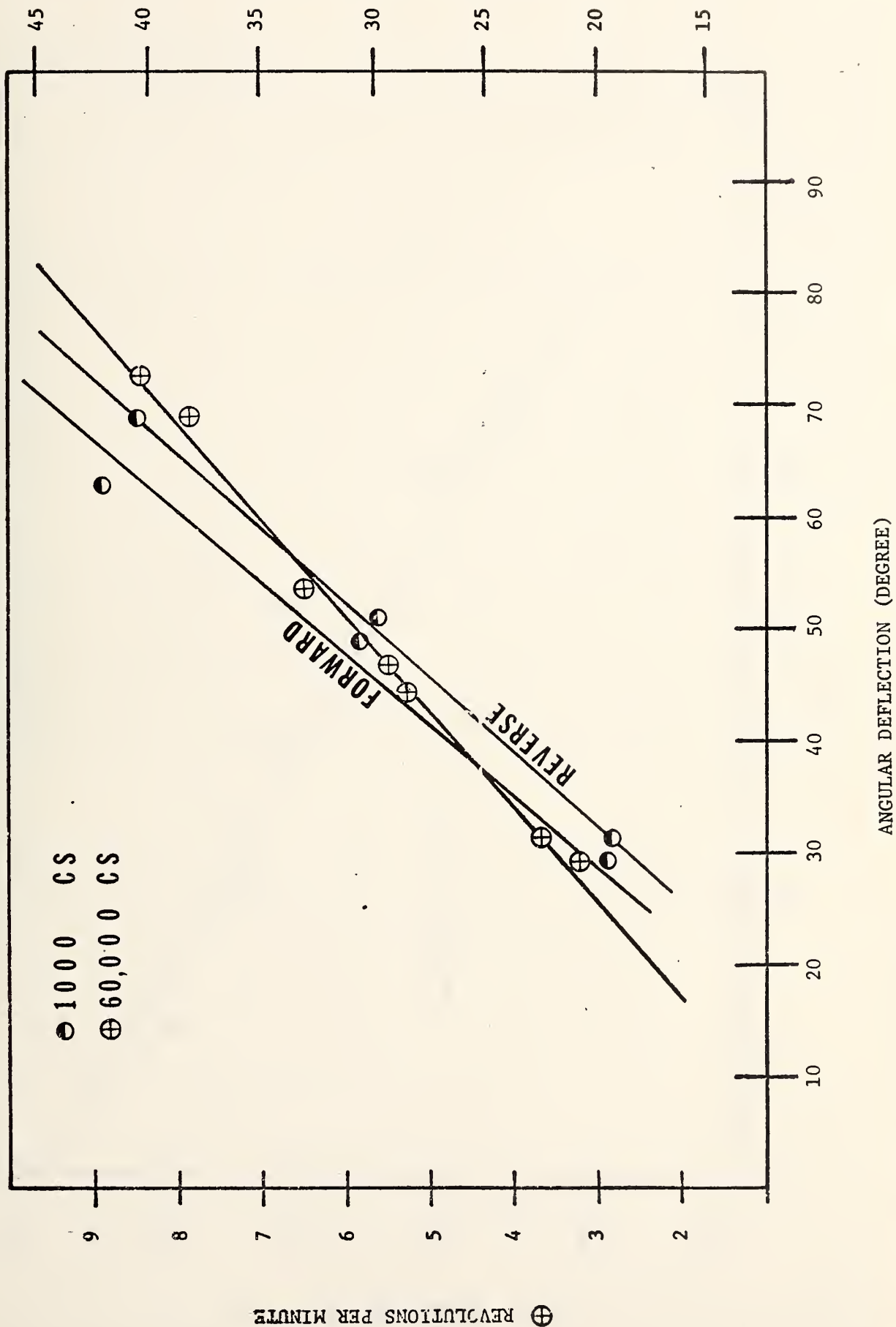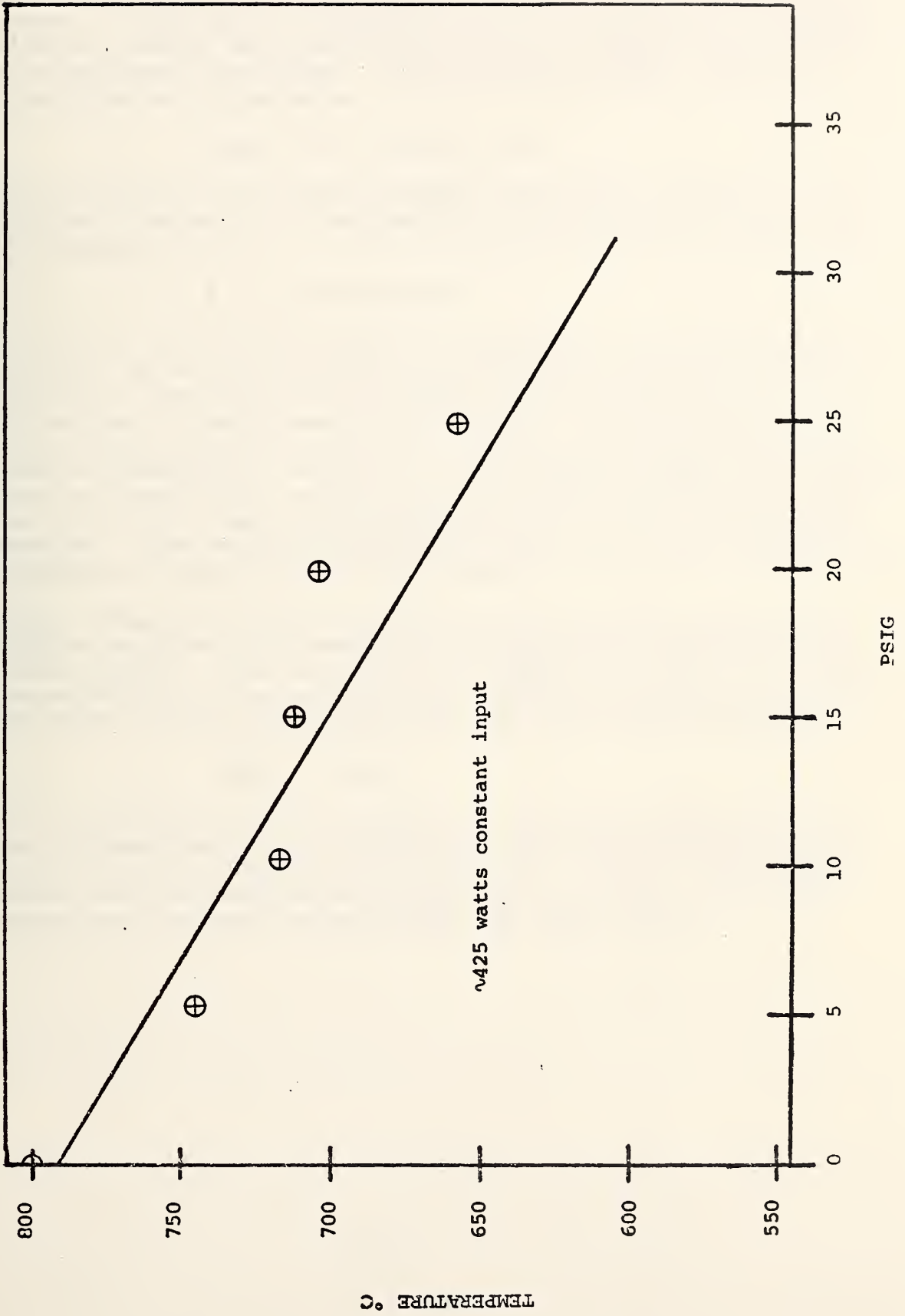
Figure 2. Angular deflection of torsion suspension vs rpm.

27

Figure 3. Temperature of strip heater vs pressure.

~425 watts constant input

PSIG

TEMPERATURE °C

28

c. Vaporization and Chemical Transport (J. Hastie and D. Bonnell, 313.01)

Progress: Quantitative vapor transport data have been obtained for molten Na_2SO_4 in an argon environment using our prototype platinum tube reactor. A wide range of pressures (0.15 to 0.6 atm) and temperatures (1390 K to 1650 K) were used to test reactor performance and attainment of thermodynamic equilibrium. The major vapor transport reaction in this system was determined as

$$Na_2SO_4 \; (\ell) = 2Na + SO_2 + O_2$$
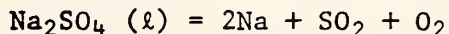
and by monitoring mass spectrometrically the partial pressures of Na, SO_2,, and O_2 values for the apparent reaction equilibrium constant could be determined, *i.e.*,

$$K_p = (pNa)^2 (pSO_2)(pO_2)$$

Also, from the so-called second law dependence of K_p on temperature, a value for the reaction enthalpy was determined as ΔH_r (1520 K) = 283±13 kcal mol^{-1}. This result is in agreement with the literature value of 287 kcal mol^{-1} (JANAF Thermochemical Tables). Similarly the absolute values of K_p agree within experimental error with the literature values based on thermodynamic equilibria. Such agreement provides good evidence that the liquid Na_2SO_4 vaporization process in an equilibrium one and that our reactor design and sampling conditions are not distrubing the reaction. These data also establish the lower sensitivity limit for the technique as 1 ppm per mole of carrier gas.

Plans: Though the present reactor design has performed satisfactorily thus far we intend to decrease the cone angle of the skimmer for aerodynamic reasons. This should allow for improved sensitivity at higher gas pressures. Following construction of this new skimmer we will test the system with NaCl by monitoring the well known vapor equilibrium:

$$2NaCl = (NaCl)_2$$
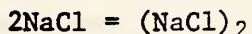
Once the modified reactor has been shown to perform satisfactorily for the relatively simple test systems, the inert argon atmosphere will be replaced by reactive gases, H_2O, H_2, SO_2, *etc.*, common to coal gasification reactors. Measurements of vapor composition as a function of temperature, pressure, and composition will then be made.

4. Failure Avoidance Programs (J. H. Smith, 312.01)

Progress: Approximately 50 additional reports of operating discrepancies and component failures in coal conversion pilot plants were received in the Failure Prevention Information Center during the current quarter. Additional information on the performance of materials in coal conversion process equipment was received from technical papers presented at the 8th Synthetic Pipeline Gas Symposium and on the properties of high temperature alloys from papers presented at the Electrochemical Society meeting.

All information on operating discrepancies, component failures, and materials performance have been classified and evaluated for technical completeness and accuracy. Detailed technical abstracts of this information have been entered into the computerized data base management system for ease of future retrieval and data dissemination. An update of the frequency of failure modes which analyses the information in this system is shown in Table 1.

Information was disseminated by supplying abstracts of information included in the data base on a weekly basis to Battelle - Columbus for use in preparation of the Materials and Components Newsletter and to other users as requested. In addition, requests for specific, detailed information were supplied to approximately 15 organizations in response to direct inquiries to the Failure Prevention Information Center. Beginning with the December 1, 1976 edition of the Materials and Components Newsletter, descriptions of operating discrepancies and component failures are referred to by NBS information item number for convenience in referring to specific failure problems.

The format was developed for two separate types of reports to be used for efficiently disseminating information from the Failure Prevention Information Center. A draft of the first abstract report on information about the use of 316 stainless steel has been completed.

A draft of a detailed summary report on erosion in coal conversion process equipment has been completed.

Plans: The information collecting phase of this task will continue as more information is received on a continuing basis from the pilot plants. Visits to operating pilot plants and failure analysis laboratories are planned to significantly augment the information collection activities and to get additional information on operating discrepancies and component failures.

The information evaluation phase of this task will include development of additional programs for use with the data base system. In addition, the information classification scheme will be revised and improved.
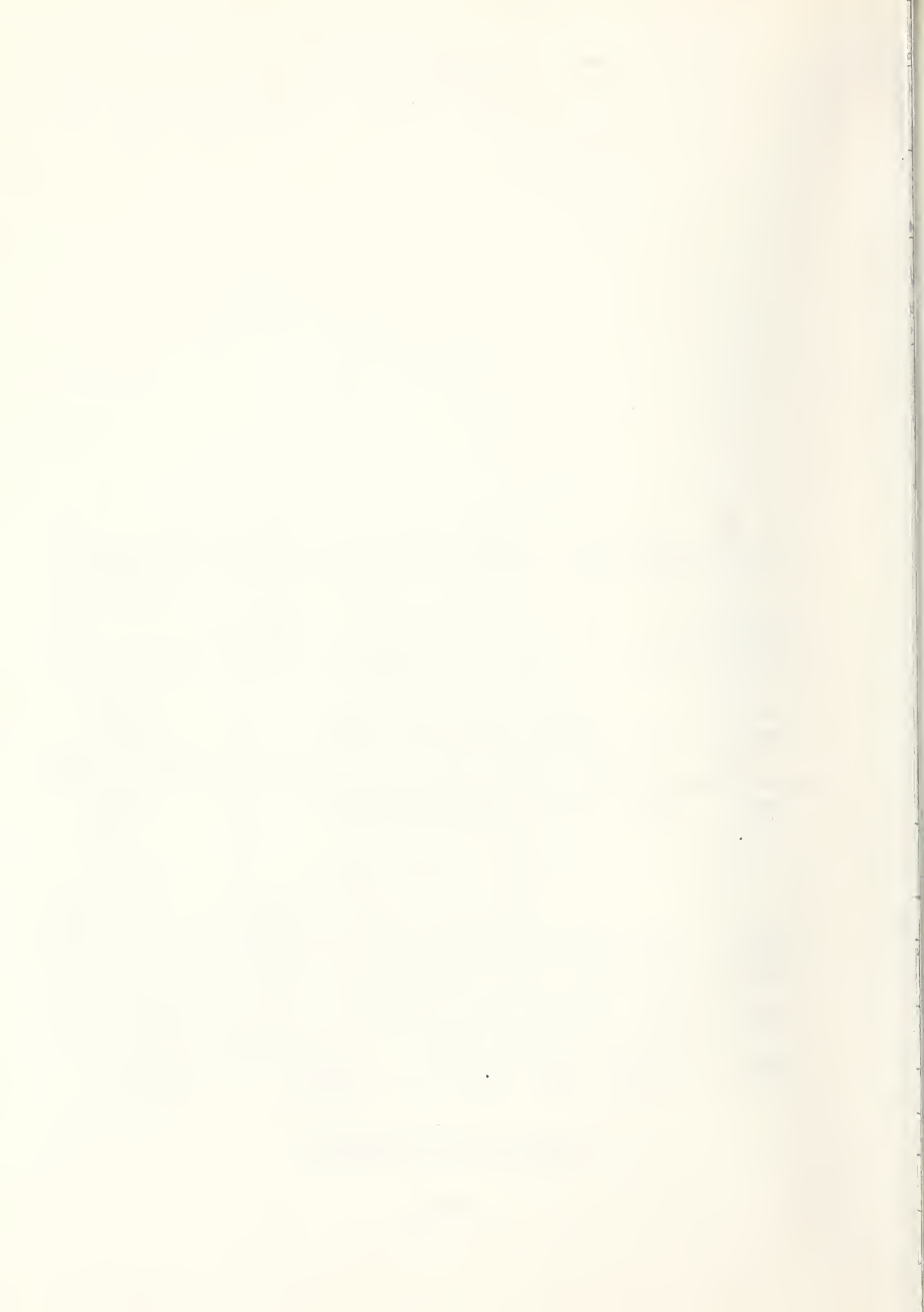
A series of detailed abstract reports are being prepared in several topical
areas including materials of construction and failure mode. A second
detailed summary report on the topic of sulfidation is being prepared and
will be completed during the next quarter.

TABLE 1

FREQUENCY OF FAILURE MODE

Cause of Incident	No. of Items	CO_2	HyGas	SRC	Synthane	Others
Undetermined	35	9	6	3	13	4
Sulfidation	21	11	7		3	
Erosion	47	9	9	8	9	21
Corrosion	118					
Pitting	4	2	2			
Dusting	4	3	3			
Carb.	9	6	2			1
General	102	32	21	9	17	26
Design Defect	31					
General	24	4	3	10	1	4
Thermal	7		3	2		2
Stresses						
SCC - CL	30	9	9		4	11
Fabrication	12					
Welding	5	1	2		1	1
Other	7	2	1		3	1
Quality Control	15	4	2		5	4

U.S. DEPT. OF COMM. BIBLIOGRAPHIC DATA SHEET	1. PUBLICATION OR REPORT NO. FE-□□□ 3800-10	2. Gov't Accession No.	3. Recipient's Accession No.

4. TITLE AND SUBTITLE

"MATERIALS RESEARCH FOR CLEAN UTILIZATION OF COAL"
Quarterly Progress Report, October 1 – December 30, 1976

5. Publication Date December 1976
6. Performing Organization Code

7. AUTHOR(S)

Samuel J. Schneider, Jr.

8. Performing Organ. Report No.

9. PERFORMING ORGANIZATION NAME AND ADDRESS

NATIONAL BUREAU OF STANDARDS
DEPARTMENT OF COMMERCE
WASHINGTON, D.C. 20234

10. Project/Task/Work Unit No.
11. Contract/Grant No. E(49-1)3800

13. Type of Report & Period Covered Quarterly Oct. 1 – Dec. 30, 1976
14. Sponsoring Agency Code Dist. Cat. UC-90C

15. SUPPLEMENTARY NOTES

16. ABSTRACT (A 200-word or less factual summary of most significant information. If document includes a significant bibliography or literature survey, mention it here.)

This progress report covers work on metal corrosion, metal erosion, ceramic deformation, fracture, erosion, and chemical degradation as related to coal gasification systems. This report also covers the failure avoidance program for ERDA coal conversion pilot plants.

17. KEY WORDS (six to twelve entries; alphabetical order; capitalize only the first letter of the first key word unless a proper name; separated by semicolons) Ceramic corrosion, ceramic erosion, ceramic fracture, chemical degradation, coal gasification material, failure avoidance, metal corrosion, metal erosion, vaporization processes

18. AVAILABILITY	☐ Unlimited	19. SECURITY CLASS (THIS REPORT)	21. NO. OF PAGES
	XX For Official Distribution. Do Not Release to NTIS NBS will not submit to NTIS; ERDA-FE will submit after approval.	UNCLASSIFIED	
	☐ Order From Sup. of Doc., U.S. Government Printing Office Washington, D.C. 20402, SD Cat. No. C13	20. SECURITY CLASS (THIS PAGE)	22. Price
	☐ Order From National Technical Information Service (NTIS) Springfield, Virginia 22151	UNCLASSIFIED	